NANO EXPRESS   **Open Access**

Lewis Basicity of Nitrogen-Doped Graphite Observed by CO$_2$ Chemisorption

CrossMark

Hisao Kiuchi[1], Riku Shibuya[2], Takahiro Kondo[2], Junji Nakamura[2], Hideharu Niwa[3,4,5], Jun Miyawaki[3,4], Maki Kawai[1], Masaharu Oshima[4] and Yoshihisa Harada[3,4*]

Abstract

The characteristics of CO$_2$ adsorption sites on a nitrogen-doped graphite model system (N-HOPG) were investigated by X-ray photoelectron and absorption spectroscopy and infrared reflection absorption spectroscopy. Adsorbed CO$_2$ was observed lying flat on N-HOPG, stabilized by a charge transfer from the substrate. This demonstrated that Lewis base sites were formed by the incorporation of nitrogen via low-energy nitrogen-ion sputtering. The possible roles of twofold coordinated pyridinic N and threefold coordinated valley N (graphitic N) sites in Lewis base site formation on N-HOPG are discussed. The presence of these nitrogen species focused on the appropriate interaction strength of CO$_2$ indicates the potential to fine-tune the Lewis basicity of carbon-based catalysts.

Keywords: CO$_2$ adsorption, Nitrogen-doped carbon, Lewis basicity, X-ray photoelectron spectroscopy, X-ray absorption spectroscopy, Infrared reflection absorption spectroscopy

Background

The problem of capturing and storing of CO$_2$ as a primary greenhouse gas must be solved to alleviate global warming. Captured CO$_2$ is typically utilized as a simple carbon-containing feedstock (C1) for generating industrially relevant organic molecules [1]. Numerous porous solid adsorbates such as zeolites [2], metal-organic frameworks [3], and mesoporous carbons [4, 5] have been proposed for the effective capture and processing of CO$_2$. Some research groups have reported that nitrogen-doped carbon materials interact more effectively with CO$_2$ than inactive carbon materials do [4–8]. Furthermore, they are also expected as promising electrocatalysts for CO$_2$ and oxygen reduction reaction [8, 9]. Accordingly, the nitrogen doping of carbon materials is expected to be an effective processes to enhance CO$_2$ storage capacity and CO$_2$ reactivity. CO$_2$ is a weak Lewis acid with an electropositive carbon atom that can detect nitrogen-doping-induced basic sites on carbon materials [10, 11]; this detection is classified as a Lewis acid/base reaction.

For practical uses of CO$_2$ adsorbents or catalysts, it is important to balance effective capturing and reduction reaction. A theoretical CO$_2$ adsorption mechanism has been proposed for the catalysts and capturing materials currently in use. For example, hydrogen bonds may form between the surface functional groups and the oxygen atoms of a CO$_2$ molecule [6]; pyridonic nitrogen species may act as anchors for CO$_2$ capture [7]; lone-pair electrons of pyridinic nitrogen may be active for CO$_2$ reduction [8]. However, detailed experimental information regarding the chemical state and geometry of adsorbed CO$_2$ on nitrogen-doped carbon materials is scarce, which hinders the design of effective, highly selective CO$_2$ capturing materials and catalysts for CO$_2$ reduction.

In this study, we investigated the adsorption properties of CO$_2$ on nitrogen-doped graphite (N-HOPG), synthesized using low-energy nitrogen-ion sputtering, using X-ray photoelectron spectroscopy (XPS), angle-resolved X-ray absorption spectroscopy (XAS), and infrared reflection-absorption spectroscopy (IRAS). Using the highly graphitized model N-HOPG with selective nitrogen doping, we discuss the possible contribution of nitrogen components to the formation of Lewis base sites on N-HOPG.

* Correspondence: harada@issp.u-tokyo.ac.jp
[3]The Institute for Solid State Physics (ISSP), the University of Tokyo, Kashiwa, Chiba, Japan
[4]Synchrotron Radiation Research Organization, the University of Tokyo, Kashiwa, Chiba, Japan
Full list of author information is available at the end of the article

Kiuchi et al. Nanoscale Research Letters (2016) 11:127

Page 2 of 7

Methods

A cleaved highly oriented pyrolytic graphite (HOPG, PGCSTM, Panasonic Inc.) plate was annealed at 1000 K for 30 min in an ultra-high vacuum (UHV) ($< 5 \times 10^{-7}$ Pa), sputtered with 8×10^{13} nitrogen ions cm^{-2} at 200 eV (equivalent to 2 % nitrogen relative to the surface carbon atoms) at 300 K using an ion gun (OMI-0730, Omegatron Inc.), and annealed again at 1000 K for 1 h for surface cleaning [12].

XPS measurements were performed at BL27SU in a third-generation synchrotron radiation facility SPring-8 using a photoelectron analyzer (PHOIBOS 150, SPECS). The typical base pressures for the measurement and preparation chambers were 4×10^{-8} and 3×10^{-7} Pa, respectively. The incident photon energy and the photoemission angle were 850 eV and 45°, respectively. The total energy resolution of the XPS was 230 meV. Samples were scanned with the incident photon beam at a rate of 0.4 μm s^{-1} to reduce the radiation damage to the adsorbed molecules. The binding energies were calibrated using the Au $4f_{7/2}$ (binding energy = 84.0 eV) peak of an evaporated gold as a reference. The N 1s spectra were fitted with the Voigt function (1.2 and 0.25 eV Gaussian and Lorentzian widths, respectively) as well as background subtraction using the Shirley method. The normalized intensity of each peak was calculated by multiplying the integrated intensity and the cross section of each element. N/C and O/C ratios were calculated by dividing the normalized intensities of the N 1s and O 1s spectra by that of C 1s spectrum, respectively. The surface nitrogen density was estimated by an assumption that nitrogen atoms are located only at the first graphite layer of HOPG. When we take into account the attenuation of photoelectrons in the bulk region, the contribution to the photoelectron from the first layer is calculated by $1 - \exp(-d/\lambda \cos\theta)$ where d is the interlayer distance, λ is the inelastic mean free path, and θ is the photoemission angle. In the present case for the C 1s XPS spectrum of graphite, this value is estimated to be 0.33 where d is 3.354 Å, λ is 11.77 Å [13] at 561 eV of kinetic energy which is obtained by subtracting the core level of C 1s (~284 eV) and work function of graphite (4.6 eV) [14] from the incident photon energy $h\nu$ = 850 eV, and θ is 45°. Therefore, the surface nitrogen and the adsorbed CO_2 densities (ML) are estimated by dividing the normalized intensities of the N 1s and O 1s XPS spectra by one third of that of the C 1s spectrum, respectively. Here, the number of the 1 ML nitrogen atoms is defined as that of the carbon atoms at the first graphite layer (3.82×10^{15} atoms cm^{-2}). The number of the adsorbed 1 ML CO_2 molecules is also defined as that of the carbon atoms at the first graphite layer and to get the number of CO_2 molecules, the estimated value from O 1s XPS should be divided by 2 since

CO_2 is composed of two oxygen atoms and one carbon atom.

N 1s and O 1s XAS spectra were measured by the partial electron yield (PEY) mode at BL27SU. The XAS spectra were collected by setting the angle θ between the incident X-ray beam axis and the surface normal to 0°, 45°, and 70°. The energy resolution of XAS had a lower limit below 100 meV.

The N-HOPG was annealed at 1000 K for 30 min in the preparation chamber to remove the initially adsorbed gas before the XPS and XAS measurements were performed. The sample was exposed to CO_2 at 300 K for 2500 s at 5.3×10^{-4} Pa, corresponding to 10,000 L in volume.

IRAS measurements were performed in grazing-angle reflection geometry both before and after CO_2 adsorption at 300 K to investigate the configuration of the adsorbed CO_2. In order to estimate the amount of the adsorbed CO_2, temperature-programmed desorption (TPD) was performed between 300 and 700 K, with CO_2 adsorption at 300 K. Both the IRAS and TPD experiments were performed in the same UHV (3×10^{-8} Pa) chamber.

Results and Discussion

Figure 1a shows the C 1s XPS spectra of HOPG and N-HOPG. The spectral intensities are normalized to the peak areas. The nitrogen ion sputtering causes the C 1s peak to broaden and introduces the C=N bond peak at 285.6 eV [15]. Figure 1b shows the N 1s XPS spectrum of N-HOPG. The N/C ratio and surface nitrogen density are calculated to be 0.0042 and 0.013 ML, respectively. The spectrum is fitted with four Voigt functions corresponding to each nitrogen component, denoted as pyridinic N (398.0 eV), cyanide N (399.9 eV), center N (401.0 eV), and valley N (401.9 eV). The terminology of the nitrogen components used hereafter is represented in Fig. 1c. Pyridinic N is connected to two carbon atoms and exists either at graphite edges or in the basal plane of graphite with a monovacancy [16]. Cyanide N has triple bonds between the nitrogen and carbon atoms [17]. Both center N and valley N are graphitic N connected to three carbon atoms, existing in the graphite basal plane, and at graphite zigzag edges or vacancy sites, respectively [18, 19]. The detailed peak assignment of each component was discussed in our previous report [12]. The estimated amount of each nitrogen component from the fitting results is summarized in Table 1; center N is the most prevalent, followed by valley N and pyridinic N.

Figure 2a shows the estimated area intensity of the mass 44 (CO_2) peak as a function of CO_2 exposure obtained by the TPD measurements. The saturation amount of adsorbed CO_2 on N-HOPG is near 10,000 L;

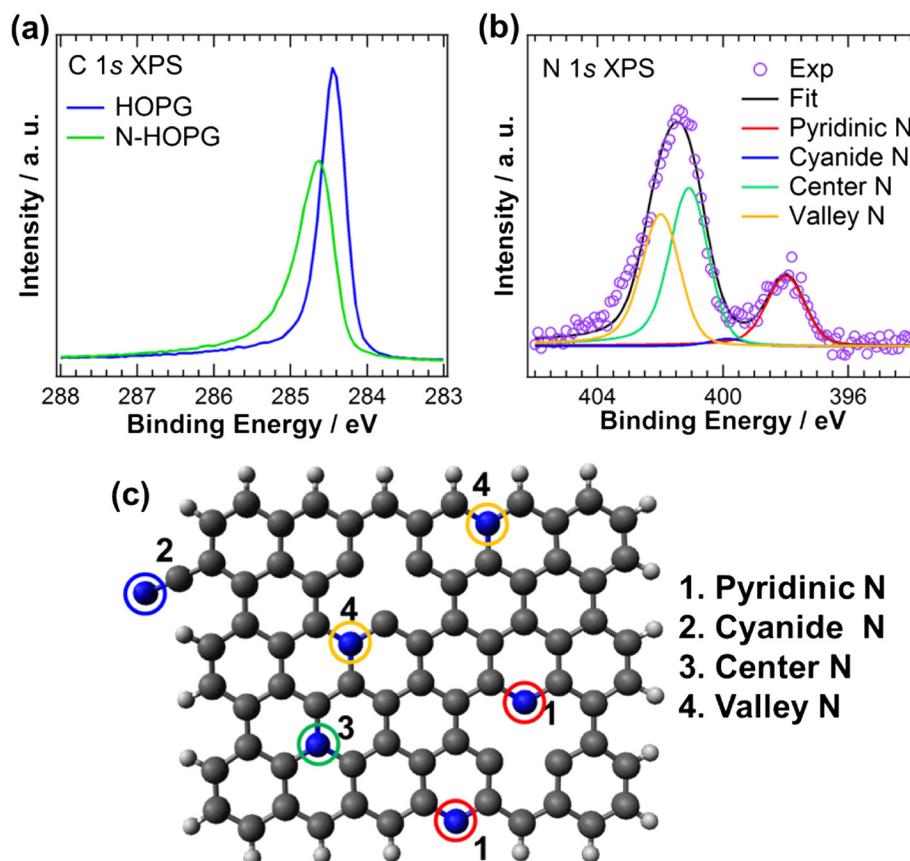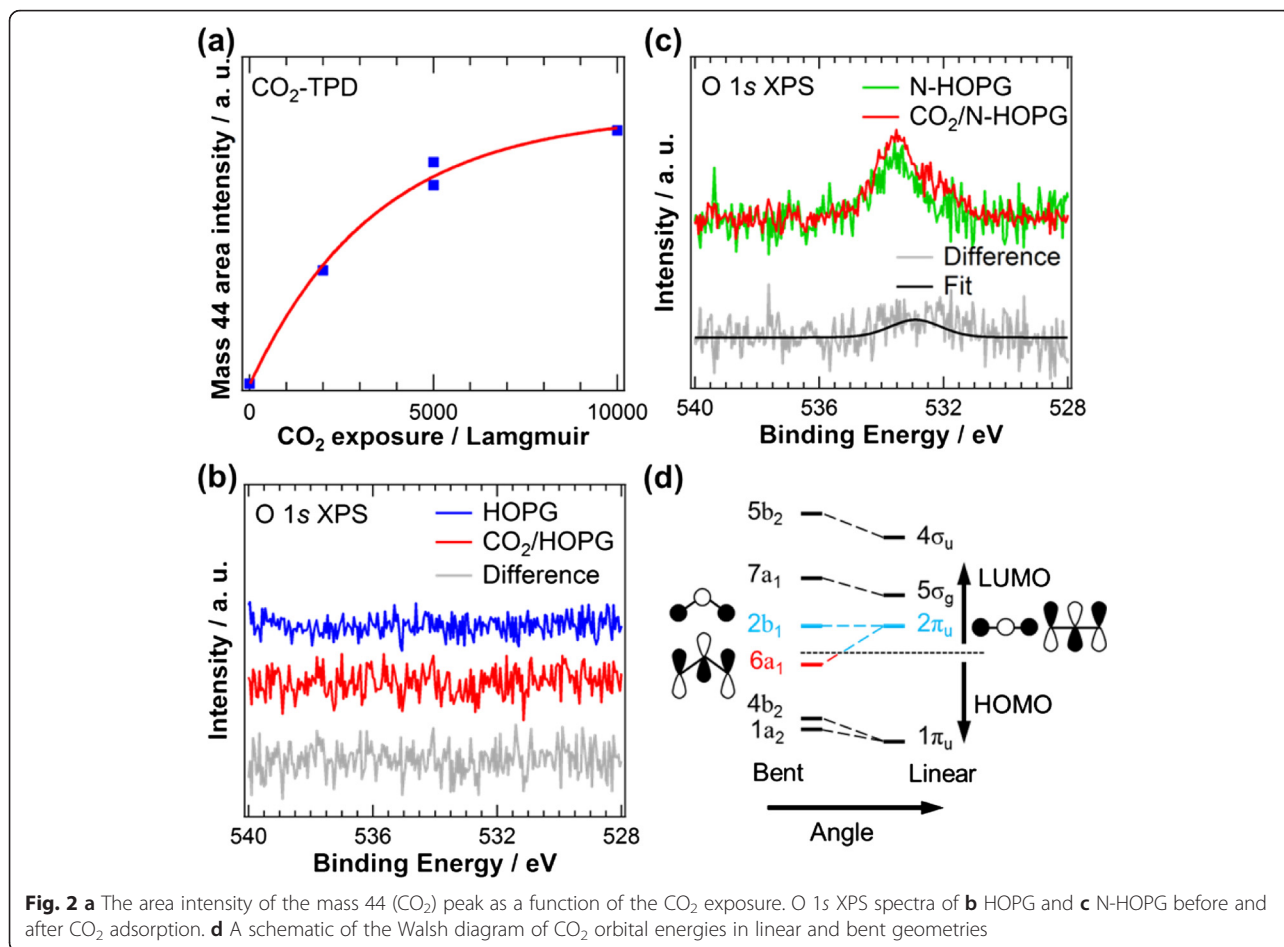Kiuchi *et al. Nanoscale Research Letters* (2016) 11:127

Page 3 of 7

Fig. 1 XPS spectra of HOPG and N-HOPG before CO_2 adsorption. **a** C 1s XPS. **b** N 1s XPS. **c** A schematic of each nitrogen configuration in N-HOPG. Hydrogen, carbon, and nitrogen atoms are represented by *white*, *black*, and *blue balls*, respectively

this amount was used for the XPS and XAS measurements. A clear CO_2 desorption peak is observed between 320 and 400 K, which approaches the temperature of CO_2 desorption for nitrogen-doped graphite model catalysts [20]. In addition, the amount of the adsorbed CO_2 on N-HOPG is almost constant when 5000 L CO_2 exposure was performed twice as shown in Fig. 2a, which indicates CO_2 adsorption is reversible without poisoning. In contrast, only physisorbed CO_2 was reported on HOPG, which desorbed at 83 K with the desorption energy of 20 kJ mol^{-1} [21]. Therefore, nitrogen doping forms CO_2 adsorption sites at 300 K on the HOPG surface. Figure 2b, c shows O 1s XPS spectra of HOPG and N-HOPG before and after CO_2 adsorption, respectively. A very small amount of oxygen species (O/C = 0.04 at.%) exists in N-HOPG before CO_2 adsorption, as shown in

Fig. 2c, which are not fully removed by annealing at 1000 K for 30 min. The difference spectrum in Fig. 2c shows an O 1s peak centered at approximately 533 eV caused by CO_2 adsorption on N-HOPG. The extracted O/C ratio and the adsorbed CO_2 density are calculated to be 0.00023 and 0.00035 ML, respectively, based on the procedure described in the "Methods" section. However, the difference spectrum in Fig. 2b of HOPG shows no peak related to adsorbed CO_2. Table 2 summarizes the O 1s binding energies for physisorbed and chemisorbed CO_2 on various substrates [22–27]; for physisorbed CO_2, the binding energy is distributed from 534.0 to 535.8 eV, while for chemisorbed CO_2, it ranges from 530.6 to 533 eV. The observed CO_2 binding energy at 533 eV on N-HOPG is below that of physisorbed CO_2 but within the range of chemisorption. The interaction strength of CO_2 directly estimates the degree of Lewis basicity of the N-HOPG substrate. To determine the origin of this binding energy, we discuss the electronic structure of CO_2 as presented by a Walsh diagram in Fig. 2d [28]. The lowest unoccupied molecular orbital (LUMO) of $2\pi_u$ is degenerated in the linear configuration, while it splits into $2b_1$ (perpendicular to the CO_2
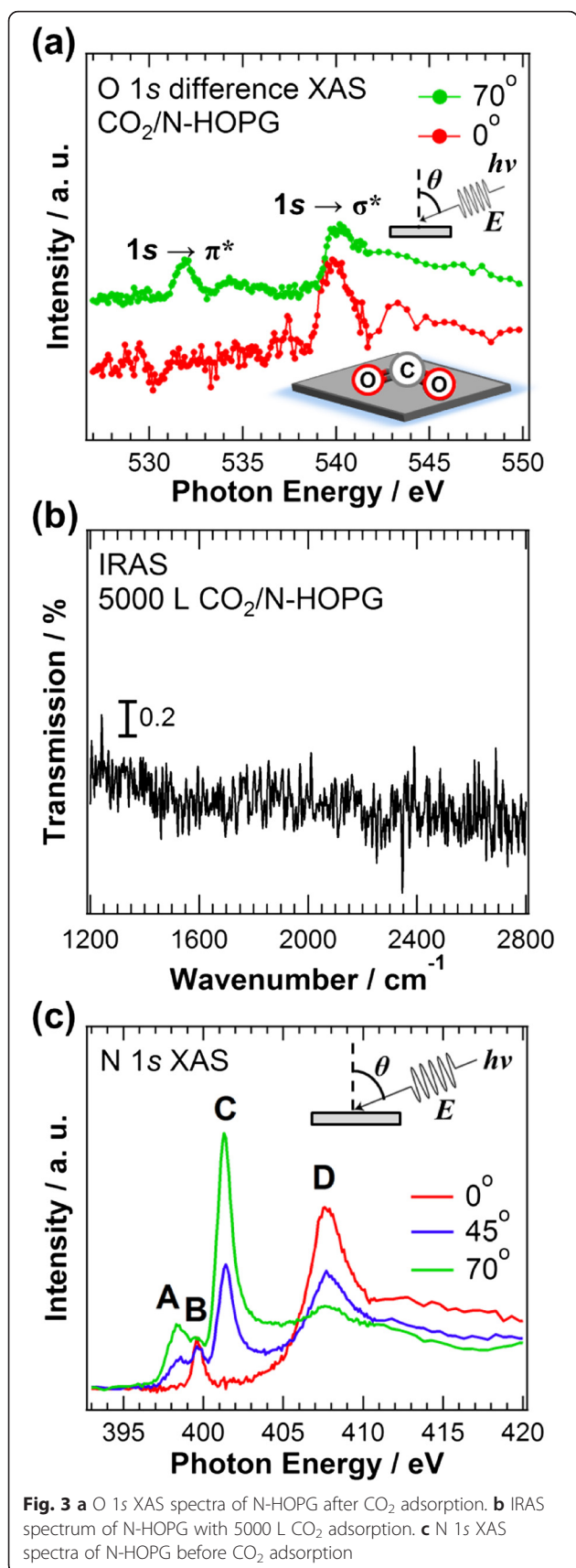
Table 1 Surface nitrogen density and relative ratio of each nitrogen component

Type of nitrogen	Pyridinic N	Cyanide N	Center N	Valley N
Nitrogen density/ML	0.0024	0.0002	0.0054	0.0045
Relative ratio/%	19	2	43	36

Kiuchi *et al. Nanoscale Research Letters* (2016) 11:127

Page 4 of 7

Fig. 2 a The area intensity of the mass 44 (CO_2) peak as a function of the CO_2 exposure. O 1*s* XPS spectra of **b** HOPG and **c** N-HOPG before and after CO_2 adsorption. **d** A schematic of the Walsh diagram of CO_2 orbital energies in linear and bent geometries

plane) and $6a_1$ (parallel to the CO_2 plane) orbitals in the bent configuration. In particular, the energy position of $6a_1$ orbital sharply decreases upon bending. In the bent configuration, this low-energy $6a_1$ orbital is occupied by electrons charge-transferred from the substrate and stabilizes the adsorbed CO_2 molecules on N-HOPG. Thus, the charge transfer from the substrate to the $6a_1$ orbital in the bent configuration weakens the strength of CO bonds, causing the O 1*s* core level shift of CO_2 to the

lower binding energy at approximately 533 eV. This result also provides evidence for the presence of Lewis base sites in the graphite system caused by the doped nitrogen.

In order to reveal the orientation of the adsorbed CO_2 on N-HOPG, angle-resolved XAS was performed. Figure 3a shows the O 1*s* XAS spectra of N-HOPG after CO_2 adsorption for different incident angles θ, where the background XAS profile obtained before CO_2

Table 2 O 1*s* binding energies for physisorbed and chemisorbed CO_2 on various substrates

Substrate	O 1*s* binding energy/eV		Ref.
	Physisorption (CO_2)	Chemisorption ($CO_2^{\delta-}$)	
Ni(110)	534.7	531.1	[22]
Ni(110)	534	530.6	[23]
Fe(poly)	535	531	[22]
Cr_2O_3(0001)	–	532.5	[24, 25]
K doped Rh(111)	534.7	532.8	[26]
K doped Mo_2C	535.8	533	[27]
N doped HOPG	–	533	This work

Kiuchi *et al. Nanoscale Research Letters* (2016) 11:127

Page 5 of 7

Fig. 3 a O 1*s* XAS spectra of N-HOPG after CO_2 adsorption. **b** IRAS spectrum of N-HOPG with 5000 L CO_2 adsorption. **c** N 1*s* XAS spectra of N-HOPG before CO_2 adsorption

adsorption is subtracted. The σ* (540 eV) and π* (532 eV) peaks are enhanced at surface normal (0°) and grazing (70°) incidence, respectively. The observed π* orbital would be derived from the $2b_1$ orbital (perpendicular to the CO_2 plane) caused by the splitting of CO_2 LUMO orbitals. Therefore, this polarization dependence of O 1*s* XAS indicates that the CO_2 molecules are lying flat on the N-HOPG surface. Although the energy position of the $6a_1$ orbital sharply decreases upon bending, the energy position of the $2b_1$ orbital remains nearly constant relative to that of the $2\pi_u$ orbital, as shown in Fig. 2d. The observed π* peak is ~2.8 eV lower than the π* peak ($2\pi_u$ orbital) for the gas-phase linear CO_2 at 534.8 eV [29], mainly because of the observed chemical shift of the O 1*s* core level in XPS, as discussed above.

The IRAS spectrum in Fig. 3b also supports the above CO_2 configuration; considering the selection rule of IRAS, the absence of peaks at approximately 1200–1300 cm^{-1} and 1600 cm^{-1}, expected for the symmetric and asymmetric OCO-stretching modes of the bent $CO_2^{\delta-}$ carboxylate with its molecular plane perpendicular to the surface [25], suggests the CO_2 to be lying flat on the surface. Both the O 1*s* XAS spectra and the IRAS spectrum of the N-HOPG support this configuration of the adsorbed CO_2.

Figure 3c shows the N 1*s* XAS spectra of the N-HOPG before CO_2 adsorption for different incident angles of 0°, 45°, and 70°. The spectra are normalized according to the intensity at 430 eV. Three sharp peaks in the π* region can be assigned to pyridinic N (A), cyanide N (B), and graphitic N (center N and valley N) (C) [12, 30]. A peak at 407.5 eV corresponds to the σ* state of the nitrogen components. The intensities of the pyridinic and graphitic N change with the X-ray incident angles, indicating that these components are incorporated into the planar graphite lattice via substitution [31]. The cyanide N, however, does not show any polarization dependence, suggesting multiple directions of the C≡N configuration. Since the adsorbed CO_2 also shows a highly oriented (lying flat) configuration, CO_2 adsorption sites should be introduced in the vicinity of the highly oriented pyridinic and graphitic N (center N and valley N).

Based on the Lewis acid/base-interaction picture, several research groups have reported possible mechanisms of CO_2 adsorption and reduction on nitrogen-doped carbon materials as follows: (1) hydrogen bonds forming between the carbon surface and oxygen atoms in a CO_2 molecule [6], (2) pyridonic N species as anchors for CO_2 capture [7], (3) a lone-pair electron located at a nitrogen atom [8], and (4) a localized electronic state of the graphite surface modified by doped nitrogen [20, 32–34]. The possibility of mechanism (1) can be excluded, because hydrogen atoms are much less prevalent in the large

Kiuchi *et al. Nanoscale Research Letters* (2016) 11:127

Page 6 of 7

platelet graphite used in this study than they can be in graphene flakes. Mechanism (2) can also be excluded because pyridonic N species, located at approximately 400 eV [7], are not observed in the N 1s XPS spectrum. For the presence of a lone-pair electron that interacts with CO_2, the most probable amine functional groups, located at 399.4 eV [16], are not observed because of the pyrolysis at ~1000 K in this work, but pyridinic N, which is present in this work, provides a possibility for mechanism (3) [8]. We consider that mechanism (4) is the most probable for creating the active sites for CO_2 adsorption and reduction. The pyridinic N detected in our results may work as a Lewis base and interact with CO_2. Indeed, recent scanning tunneling spectroscopy measurements have revealed the presence of an electronic structure just 370 meV below the Fermi level of several localized carbon atoms surrounding pyridinic N at monovacancy sites [33]. The observed valley N site is also expected to modify the electronic structure of the surrounding carbon atoms and induce a local density of states of ~200–400 meV below the Fermi level [34], which may also provide CO_2 adsorption and reaction sites. Therefore, the interaction sites with CO_2 in N-HOPG would be provided by the lone-pair electrons of pyridinic N or the localized π states just below the Fermi level induced by the pyridinic N and/or valley N. According to the recent report with HOPG model catalysts, pyridinic N can create Lewis base sites for CO_2 adsorption on carbon materials [20], which is consistent with our present discussion. The clear evidence of the charge transfer from the substrate and the new information on the molecular orientations of both CO_2 and nitrogen moieties on the graphite substrate provide great insight into the CO_2 adsorption mechanism, and the Lewis basicity of nitrogen-doped graphite can be directly estimated by element-specific synchrotron analyses.

Conclusions

We have investigated the adsorbed CO_2 at 300 K on N-HOPG by XPS, angle-resolved XAS, and IRAS using a model N-HOPG synthesized by a protocol developed in a previous study. The O 1s binding energy of the adsorbed CO_2 at 300 K, located at 533 eV, showed clear evidence of the Lewis basicity of N-HOPG caused by the nitrogen doped in the graphite system. The polarization dependence of the σ* and π* peaks in the O 1s XAS spectra, as well as the absence of expected IRAS signals, clearly indicates that the adsorbed CO_2 lies flat on the graphite surface and that Lewis base sites are induced by the incorporation of nitrogen in HOPG. We discussed possible CO_2 adsorption sites induced by pyridinic N and valley N species. The activity of these species as adsorption sites indicates the potential to fine-tune the Lewis basicity of a graphite substrate by controlling the prevalence of nitrogen species focused on the

appropriate interaction strength of CO_2, which can be directly estimated by the O 1s binding energy of the adsorbed CO_2. The properties of fine-tuned Lewis basicity in carbon-based materials can be applied to the field of catalysis, including the use of the materials as oxygen reduction reaction or hydrogen evolution reaction sites.

Author details

[1]Department of Applied Chemistry, the University of Tokyo, 7-3-1 Hongo, Bunkyo-ku, Tokyo 113-8656, Japan. [2]Faculty of Pure and Applied Sciences, University of Tsukuba, Ibaraki, Japan. [3]The Institute for Solid State Physics (ISSP), the University of Tokyo, Kashiwa, Chiba, Japan. [4]Synchrotron Radiation Research Organization, the University of Tokyo, Kashiwa, Chiba, Japan. [5]Present address: Graduate School of Pure and Applied Sciences, University of Tsukuba, Ibaraki, Japan.

References

1. Arakawa H, Aresta M, Armor JN, Barteau MA, Beckman EJ, Bell AT et al (2001) Catalysis research of relevance to carbon management: progress, challenges, and opportunities. Chem Rev 101:953–96
2. Choi S, Drese JH, Jones CW (2009) Adsorbent materials for carbon dioxide capture from large anthropogenic point sources. ChemSusChem 2:796–854
3. McDonald TM, Mason JA, Kong X, Bloch ED, Gygi D, Dani A et al (2015) Cooperative insertion of CO_2 in diamine-appended metal-organic frameworks. Nature 519:303–8
4. Wang Y, Zou H, Zeng S, Pan Y, Wang R, Wang X et al (2015) A one-step carbonization route towards nitrogen-doped porous carbon hollow spheres

Kiuchi *et al. Nanoscale Research Letters* (2016) 11:127

Page 7 of 7

with ultrahigh nitrogen content for CO_2 adsorption. Chem Commun 51: 12423–6

5. Wei J, Zhou D, Sun Z, Deng Y, Xia Y, Zhao D (2013) A controllable synthesis of rich nitrogen-doped ordered mesoporous carbon for CO_2 capture and supercapacitors. Adv Funct Mater 23:2322–8

6. Xing W, Liu C, Zhou Z, Zhang L, Zhou J, Zhuo S et al (2012) Superior CO_2 uptake of N-doped activated carbon through hydrogen-bonding interaction. Energy Environ Sci 5:7323–7

7. Sevilla M, Valle-Vigón P, Fuertes AB (2011) N-doped polypyrrole-based porous carbons for CO_2 capture. Adv Funct Mater 21:2781–7

8. Sharma PP, Wu J, Yadav RM, Liu M, Wright CJ, Tiwary CS et al (2015) Nitrogen-doped carbon nanotube arrays for high-efficiency electrochemical reduction of CO2: on the understanding of defects, defect density, and selectivity. Angew Chemie Int Ed 54:13701–5

9. Gong K, Du F, Xia Z, Durstock M, Dai L (2009) Nitrogen-doped carbon nanotube arrays with high electrocatalytic activity for oxygen reduction. Science 323:760–4

10. Auroux A, Gervasini A (1990) Microcalorimetric study of the acidity and basicity of metal oxide surfaces. J Phys Chem 94:6371–9

11. Lavalley JC (1996) Infrared spectrometric studies of the surface basicity of metal oxides and zeolites using adsorbed probe molecules. Catal Today 27: 377–401

12. Kiuchi H, Kondo T, Sakurai M, Guo D, Nakamura J, Niwa H et al (2016) Characterization of nitrogen species incorporated into graphite using low energy nitrogen ion sputtering. Phys Chem Chem Phys 18:458–65

13. Tanuma S, Powell CJ, Penn DR (2010) Calculations of electron inelastic mean free paths. IX. Data for 41 elemental solids over the 50 eV to 30 keV range. Surf Interface Anal 43:689–713

14. Takahashi T, Tokailin H, Sagawa T (1985) Angle-resolved ultraviolet photoemission spectroscopy of the unoccupied band structure of graphite. Phys Rev B 32:8317–24

15. Scardamaglia M, Amati M, Llorente B, Mudimela P, Colomer J-F, Ghijsen J et al (2014) Nitrogen ion casting on vertically aligned carbon nanotubes: tip and sidewall chemical modification. Carbon 77:319–28

16. Pels J, Kapteijn F, Moulijn J, Zhu Q, Thomas K (1995) Evolution of nitrogen functionalities in carbonaceous materials during pyrolysis. Carbon 33:1641–53

17. Jansen R, Van Bekkum H (1995) XPS of nitrogen-containing functional groups on activated carbon. Carbon 33:1021

18. Sharifi T, Hu G, Jia X, Wågberg T (2012) Formation of active sites for oxygen reduction reactions by transformation of nitrogen functionalities in nitrogen-doped carbon nanotubes. ACS Nano 6:8904–12

19. Casanovas J, Ricart JM, Rubio J, Illas F, Jiménez-Mateos JM (1996) Origin of the large N 1s binding energy in X-ray photoelectron spectra of calcined carbonaceous materials. J Am Chem Soc 118:8071–6

20. Guo D, Shibuya R, Akiba C, Saji S, Kondo T, Nakamura J. Active sites of nitrogen-doped carbon materials for oxygen reduction reaction clarified using model catalysts. Science. in press.

21. Edridge JL, Freimann K, Burke DJ, Brown WA (2013) Surface science investigations of the role of CO_2 in astrophysical ices. Philos Trans R Soc A Math Phys Eng Sci 371:20110578

22. Illing G, Heskett D, Plummer EW, Freund H-J, Somers J, Lindner T et al (1988) Adsorption and reaction of CO_2 on Ni{110}: X-ray photoemission, near-edge X-ray absorption fine-structure and diffuse leed studies. Surf Sci 206:1–19

23. Ding X, De Rogatis L, Vesselli E, Baraldi A, Comelli G, Rosei R et al (2007) Interaction of carbon dioxide with Ni(110): a combined experimental and theoretical study. Phys Rev B 76:195425

24. Kuhlenbeck H, Xu C, Dillmann B, Haßel M, Adam B, Ehrlich D et al (1992) Adsorption and reaction on oxide surfaces: CO and CO_2 on Cr_2O_3(111). Berichte Der Bunsengesellschaft Für Phys Chemie 96:15–27

25. Seiferth O, Wolter K, Dillmann B, Klivenyi G, Freund HJ, Scarano D et al (1999) IR investigations of CO_2 adsorption on chromia surfaces: Cr_2O_3 (0001)/Cr(110) versus polycrystalline α-Cr_2O_3. Surf Sci 421:176–90

26. Kiss J, Révész K, Solymosi F (1988) Photoelectron spectroscop1c studies of the adsorption of CO_2 on potassium-promoted Rh(111) surface. Surf Sci 207: 36–54

27. Bugyi L, Oszkó A, Solymosi F (2000) Spectroscopic study on the formation of CO_2^- on K-promoted Mo_2C/Mo(100) surface. Surf Sci 461:177–90

28. Freund HJ, Roberts MW (1996) Surface chemistry of carbon dioxide. Surf Sci Rep 25:225–73

29. Maganas D, Kristiansen P, Duda L-C, Knop-Gericke A, DeBeer S, Schlögl R et al (2014) Combined experimental and ab initio multireference configuration interaction study of the resonant inelastic X-ray scattering spectrum of CO_2. J Phys Chem C 118:20163–75

30. Schiros T, Nordlund D, Pálová L, Prezzi D, Zhao L, Kim KS et al (2012) Connecting dopant bond type with electronic structure in N-doped graphene. Nano Lett 12:4025–31

31. Shimoyama I, Wu G, Sekiguchi T, Baba Y (2000) Evidence for the existence of nitrogen-substituted graphite structure by polarization dependence of near-edge x-ray-absorption fine structure. Phys Rev B 62:R6053–6

32. Kondo T, Honma Y, Oh J, Machida T, Nakamura J (2010) Edge states propagating from a defect of graphite: scanning tunneling spectroscopy measurements. Phys Rev B 82:153414

33. Kondo T, Casolo S, Suzuki T, Shikano T, Sakurai M, Harada Y et al (2012) Atomic-scale characterization of nitrogen-doped graphite: effects of dopant nitrogen on the local electronic structure of the surrounding carbon atoms. Phys Rev B 86:035436

34. Huang SF, Terakura K, Ozaki T, Ikeda T, Boero M, Oshima M et al (2009) First-principles calculation of the electronic properties of graphene clusters doped with nitrogen and boron: analysis of catalytic activity for the oxygen reduction reaction. Phys Rev B 80:235410